FASTC-ID(RS)T-0619-92

FOREIGN AEROSPACE SCIENCE AND TECHNOLOGY CENTER

DIAGNOSIS OF PLASMA STATES IN X-RAY LASER EXPERIMENTS

by

Yang Shangjin, Cai Yuqin, Chunyu Shutai

HUMAN TRANSLATION

FASTC-ID(RS)T-0619-92 8 October 1992

DIAGNOSIS OF PLASMA STATES IN X-RAY LASER EXPERIMENTS

By: Yang Shangjin, Cai Yuqin, Chunyu Shutai

English pages: 13

Source: Unknown; pp. 73-78

Country of origin: China
Translated by: Leo Kanner Associates
F33657-88-D-2188
Requester: FASTC/TATD/Jeff Bacso
Approved for public release; Distribution unlimited.

PREPARED BY:

TRANSLATION DIVISION
FOREIGN AEROSPACE SCIENCE AND TECHNOLOGY CENTER
WPAFB, OHIO

GRAPHICS DISCLAIMER

All figures, graphics, tables, equations, etc. merged into this translation were extracted from the best quality copy available.

DIAGNOSIS OF PLASMA STATES IN X-RAY LASER EXPERIMENTS

Yang Shangjin, Cai Yuqin, and Chunyu Shutai
China Academy of Engineering Physics

Abstract

At an LF-12 laser installation, an Nd glass laser of approximately 1.5 ns pulse width with 500 to 600 J was focussed into a line 120 micrometers wide and 20 mm long and then onto a 1.5 mm thick germanium plane target. A plane crystal spectrograph (wavelength measurement range was between 0.6 and 0.9 nm) with a spatial resolving power was placed in the target chamber to diagnose the germanium plasma state. The corresponding intensity ratio between the quasi-Ne ion spectral lines with 2p-nd (n greater than or equal to 4) energy level transition was used to estimate the plasma electron temperature at 400 to 600 eV. In the laboratory, the measured line spectrum was mainly generated by quasi-Ne Ge XXIII ions; next were the spectral lines generated by quasi-F Ge XXIV ions; the spectral lines generated by quasi-Na Ge XXII ions were relatively weak. In addition, the axial-direction distribution uniformity of linear plasma, and the lateral-direction distribution characteristics of ions were provisionally observed.
Keywords: X-ray laser and plasma parameters.

I. Introduction

Research on X-ray lasers is very important for plasma state diagnostics [1]. From the principle of X-ray laser generation, we know the following: to obtain an X-ray laser with higher gain, the gain medium for generating an X-ray laser should satisfy

certain conditions. In other words, after irradiation with a linear focusing laser and within a certain time period, the gain medium will form a plasma with specific electron temperatures, electron density, and ion abundance with uniform distribution within a definite region. In experiments, by diagnostics of the plasma state, the optimal conditions for generating an X-ray laser can be realized; in addition, the theoretical models can be examined and X-ray laser research can be promoted for extensive development.

At the largest high-power laser LF-12 installation in China, for the first time the authors conducted the quasi-Ne germanium X-ray laser experiments with collisional excitation as the pumping mechanism. When they obtained a yield of five X-ray spectral lines with stimulated radiation amplification [2], the authors measured the linear plasma parameters by using a plane crystal spectrograph with a spatial resolving power to measure the linear plasma parameters. The measured linear plasma parameters can provide valuable reference data for qualitative improvements in the pumping laser beam, and for the general design of X-ray laser experiments in the future.

II. Simplified Plasma Model [3, 4]

For certain plasmas, the optical thickness is very thin and the radiation field density is very low, therefore the process of photoionization and photo-caused laser production can be neglected; radiation and absorption is not in balance. However, since the particle density is still large enough with frequent collisions, the so-called thermal equilibrium can still be attained. At this time, the distribution of particle states can be described with the Maxwell-Boltzmann distribution and the Saha equation. In X-ray laser experiments, particle density is incapable of satisfying the above-mentioned conditions (Ne is approximately 10^{20} cm^{-3}). However, the approximate local thermal

equilibrium can be attained among several excited states at some energy level (n greater than or equal to 4). In other words, there is a partial local thermal equilibrium (PLTE). Therefore, among various energy levels of the identical ionization in the plasma, the number of particles can still be expressed with the Boltzmann relationship:

$$\frac{N_n}{N_0} = \frac{g_n}{g_0} \exp(-E_{0n}/T_e) \qquad (1)$$

In the equation, N_0 and N_n indicate, respectively, the number of particles in the ground state and the n excited state; g_0 and g_n are the corresponding statistical weights; E_{on} is the excitational energy from the ground state to the excited; and T_e is the electron temperature.

For plasma linear radiation, generally only the spontaneous transitions are considered. If the plasma is homogeneous, the surface brightness of any spectral line is:

$$B_{nm} = \frac{1}{4\pi} E_{nm} N_n A_{nm} D \qquad (\mathrm{W \cdot m^{-2} \cdot sr^{-1}}) \qquad (2)$$

A_{nm} stands for the spontaneous transition probability from the n state to the m state; D is the plasma thickness along the observation direction; and E_{nm} is the photon energy.

By using Eqs. (1) and (2), we can obtain the relationship between the intensity ratio and the electron temperature of the spectral lines generated in two transitions of ions with the same ionization as:

$$\frac{B_{nm}}{B_{kB}} = \frac{E_{nm}}{E_{kB}} \cdot \frac{A_{nm}}{A_{kB}} \cdot \frac{g_n}{g_k} \exp(-E_{Bm}/T_e) \qquad (3)$$

In the equation, $E_{Bm} = E_{0n} - E_{0k}$.

According to the PLTE approximation, only by measuring the

intensity ratio of two spectral lines (selecting the intensity ratio of spectral lines with a close relationship to electron temperature), and by substituting the parameters E, g, and A (among others) in Eq. (3), then the electron temperature T_e of the plasma can be obtained.

Similarly, the relationship between the intensity ratio and the electron temperature of two spectral lines generated by ions of different ionization is:

$$\frac{B_{nm}^{z+1}}{B_{kB}^{z}} = \frac{E_{nm}^{z+1}}{E_{kB}^{z}} \cdot \frac{A_{nm}^{z+1}}{A_{kB}^{z}} \cdot \frac{g_n^{z+1}}{g_n^{z}} \cdot \frac{g_0^{z}}{g_0^{z+1}} \cdot \frac{N_0^{z+1}}{N_0^{z}} \exp\left(-\frac{E_{0n}-E_{0k}}{T_e}\right) \qquad (4)$$

When T_e is known, the ion abundance ratio between z + 1 order ions and z order ions can be computed as:

$$\eta = \frac{N_0^{z+1}/g_0^{z+1}}{N_0^{z}/g_0^{z}} = \frac{B_{nm}^{z+1}}{B_{kB}^{z}} \cdot \frac{E_{kB}^{z}}{E_{nm}^{z+1}} \cdot \frac{A_{kB}^{z}}{A_{nm}^{z+1}} \cdot \frac{g_k^{z}}{g_n^{z+1}} \exp(E_{Bm}/T_e) \qquad (5)$$

III. Experiment

The layout of the experimental installation is shown in Fig. 1: the laser wavelength is 1.05 micrometers; the laser pulse width (FWHM) is approximately 1.5 ns; the variation range of laser energy is 450 to 600 J; the width of linear focusing is approximately 120 micrometers; and the linear length is 20 mm. The X-ray laser target is a thick block plane germanium target; the target surface was buffed to ensure that the flatness of the target surface satisfies the experimental requirements. Variations in target length are, respectively, 8 mm, 12 mm, 14 mm, 16 mm, and 18 mm. By using a glancing incident grating spectrograph for the measurements, the intensity of X-ray spectral lines varies with the target length.

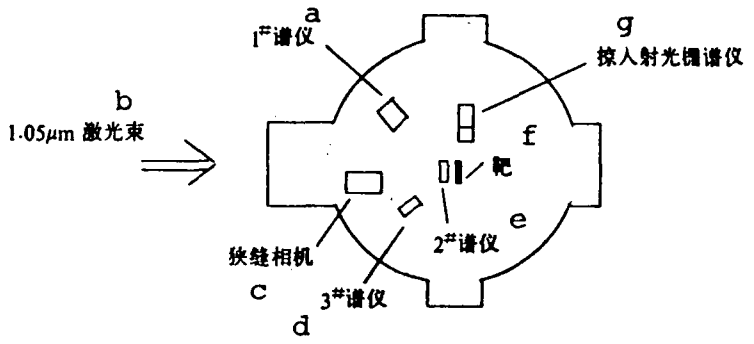

Fig. 1. Layout of experimental installation
KEY: a - No. 1 spectrograph b - 1.05 micrometers laser beam c - narrow-slit camera d - No. 3 spectrograph e - No. 2 spectrograph f - target g - glancing incident grating spectrograph

Three plane crystal spectrographs are employed to measure the linear plasma parameters: the No. 1 spectrograph is installed in the right front side of the target to form an angle of 45° with the target surface at a distance of 16 cm from the target center. The slit width of the spectrograph is 500 micrometers and the diffraction crystal is TAP (2d = 2.576 nm). The spectrograph was used to measure the axial-direction distribution homogeneity of the plasma. The No. 2 spectrograph was installed at the front lower side to form an approximate angle of 27° with the target surface. The diffraction crystal is KAP (2d = 2.663 nm); and the slit width is 50 micrometers (the slit is parallel to the focusing line). This spectrograph was used to measure the distribution of plasma along the direction of the incident laser. The No. 3 spectrograph was installed at the left front of the target, approximately 5 cm from the target surface. The deflection crystal is KAP. The slit is normal to the linear focusing and its width is 1 mm; this spectrograph was used to measure the entire radiation spectrum (0.6 to 1.0 nm) of the plasma, and to make fiducial marks on the X-ray negative. The X-ray response curve that is obtained can be used to revise the relative intensity ratios of the spectral lines. At the front

upper side of the target and 16 cm from the target center, a slit camera is placed to monitor the width of the incident laser focusing lines.

IV. Measurement Results

1. Response characteristic curve on X-ray negative

A single-order trapezoidal-shaped aluminum filter plate was placed at the incidence window of the negative film case of the No. 3 crystal spectrograph. Because of different thicknesses of various order layers of the filter plates, intensities of X-rays incident to the negative were altered. If there are M spectral lines within a narrower energy region, and there is little influence on the shape of the response characteristic curves on the negative due to the wavelength of light exposure, this can be neglected. After M spectral lines penetrated the M order layers of the filter plate, there were M x N spectral lines at different intensities upon exposure of the negative to light. Mathematical processing was then performed for the relative intensities of M x N spectral lines and the corresponding blackness densities, a more ideal response characteristic line on the negative can be obtained.

In this experiment, at the front window of the negative film case, a three-order layer aluminum filter plate was placed. By utilizing the plasma radiation X-ray spectrum generated when the laser beam struck the germanium plane target, the wavelength was between 0.6 and 0.5 nm; the four spectral lines that were selected were as follows: $GeXXIII\ 2s^22p^6-2p^54d\ (0.7205\ nm)$, $GeXXIV\ 2s^22p^5-2p^44d\ (0.6727nm)$, $GeXXIII\ 2s^22p^6-2p^55d\ (0.6464nm)$, $GeXXIII\ 2s^22p^6-2p^56d\ (0.6272nm)$. The graduation of response characteristic curve (by using a Kodak AA5 type negative made in the United States) is shown in Fig. 2.

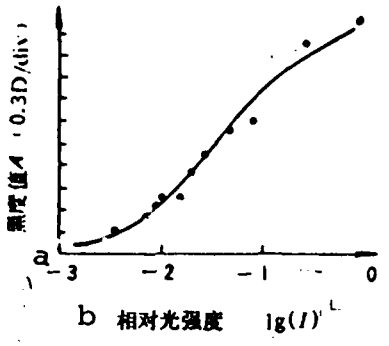

Fig. 2. Response curve using Kodak AA5 negative made in the United States
KEY: a - blackness value A (0.3 D/div)
b - relative light intensity lg(I)

2. Electron temperature

Measured with the plane crystal spectrograph, the X-ray spectral lines of plasma radiation generated by the laser beam incident at the germanium plane target are shown in Fig. 3. When the laser power density at the target surface was (0.8 to 1.2) x x 10^{13} W/cm^2 and when the range of spectral lines recorded with the plane crystal spectrograph was between 0.6 and 1.0 nm, from Fig. 3 the spectral lines in the spectrum were generated mainly by quasi-Na Ge XXIII ions; next came the spectral lines generated by quasi-F Ge XXIV ions; and the spectral lines generated by the quasi-Na Ge XXII ions were very faint.

By utilizing the model approximation of local thermal equilibrium, in other words, it is assumed that partial local thermal equilibrium (PLTE) exists between the energy levels $2p^6$ - $2p^5nd$ (n greater than or equal to 4) of the quasi-Ne Ge XXIII ions for the generation of spectral lines, substitute the parameters A,E, and g [5] into Eq. (3). By using the relative intensity ratios of the spectral lines $I(2p^6-5d)/I(2p^6-4d)$ and $I(2p^6-6d)/I(2p^6-5d)$ to determine the relative intensity ratio of $I(2p^5-4d)/I(2p^6-4d)$

of germanium ions, and the average electron temperature of Ge plasma, thus estimating the relative abundance ratios of quasi-F

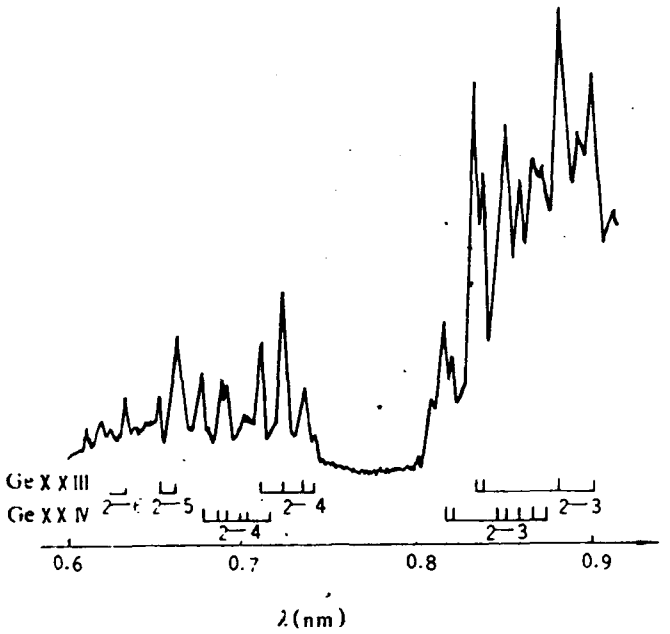

Fig. 3. Line spectrum of Ge plasma radiation

ions and quasi-Ne ions to be listed in Table 1.

TABLE 1. Electron Temperature T_e and Relative Abundance η of Germanium Plasma

a 发次	靶 b 厚 (mm)	靶 长 (mm) c	激光能量 (J) d	脉 宽 (ps) e	功率密度 (W/cm²) f	T_e (eV)	η
33	1	18.146	598.21	1312	9.25×10^{12}	387	0.365
38	1	8.4	642.06	1406	9.26×10^{12}	433	0.256
42	1	16.07	592.73	1156	1.01×10^{13}	476	0.442
46	1	18.15	475.28	1264	1.14×10^{13}	631	0.236

KEY: a - number of experiments b - target thickness, (mm) c - target length (mm) d - laser energy (J) e - pulse width (ps) f - power density (W/cm^2)

The following findings are revealed as the measurement results: the mean electron temperature is between 400 and 600 eV for the germanium plasma when an X-ray laser is generated; the relative abundance of the quasi-F ions and quasi-Ne ions is

between 0.2 and 0.35.

3. Axial-direction distribution homogeneity of plasma

The No. 1 spectrograph was used to arrive at a better observation on the axial-direction distribution status of the plasma, the electron temperature of various points in the axial direction, and the abundance value of the relative ions. These parameters are listed in Table 2. We can see from the measurement results in Table 2 that the variation in the axial-direction electron temperature along the linear plasma is as high as 35%; the variation of the relative ion abundance is as high as 33%.

TABLE 2. Measurement Results of Axial-Direction Distribution Homogeneity of Plasma
(Measurement conditions: 33 target hits; target material -- Ge; target thickness -- 1 mm; target length -- 18.15 mm; and power density -- 9.25 x x 10^{12} W/cm^2)

1 位 置	1	2	3	4	5	6	7	8
T_e(eV)	410	481	325	/	316	268	523	/
η	0.363	0.352	0.405	0.337	0.367	0.344	0.350	0.258

KEY: 1 - position

By using the axial-direction spatial resolution energy spectrum to scan along the linear focusing direction, the scanning trace is shown in Fig. 4. From Fig. 4, two different axial-direction structures of the plasma can be observed: one is a relatively fine folded structure, and the other is an irregular, inhomogeneous structure of millimeter scale. The former case is possible due to instability of linear plasma; the latter is related to the laser pulse rise time. Currently, the pulse rise time is still not fast enough (greater than 1 ns); this phenomenon can also be used with a slit camera.

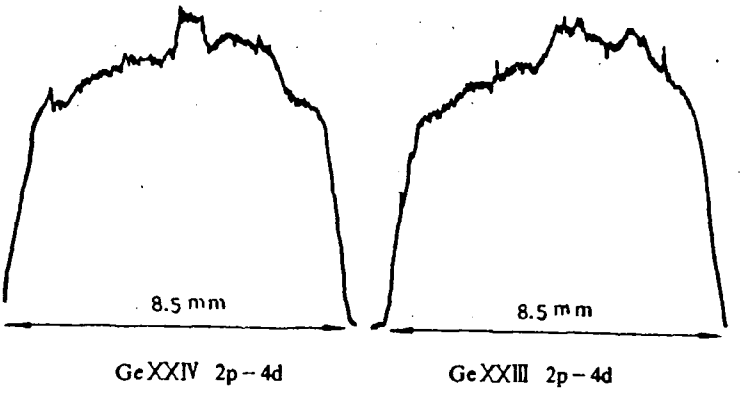

Fig. 4. Scanning trace in the linear focusing direction of Ge XXIV $2p^5$-4d and Ge XXIII $2p^6$-4d

4. Lateral-direction distribution of plasma

In X-ray laser experiments, distributions are uniform for the axial direction and the lateral direction along the linear plasma; this not only obtains the maximum gain of an X-ray laser, but also can avoid a very steep electron density gradient in the linear plasma so that refraction is generated during the propagation of an X-ray laser beam to be deviated out of the gain region [6]. In this experiment, although the slit of the crystal spectrograph is parallel to the linear focusing, spectral line broadening due to plasma source is very substantial. However, from the Ge ion linear spectrum (Fig. 3) measured with the No. 3 spectrograph, we can observe that the spectral lines generated by the $2p^6$-3d energy level transition of Ge XXIII ions generally overlap the spectral lines produced in the transition of quasi-F Ge XXIV ions $2p^5$-3d and quasi-Na Ge XXII ions. Moreover, the latter is much weaker than the former. Therefore, the line spectrum generated during point target strikes measured by the No. 2 spectrograph is the marking line, thus determining the position of spectral lines generated in the $2p^6$-3d energy level transition of quasi-Ne Ge ions, not considering the contribution of spectral lines of quasi-F and quasi-Na Ge ions. Through

observation of the spatial distribution of spectral lines produced in the $2p^6$-3d transition of quasi-Ne Ge XXIII ions, the distribution status of Ge XXIII ions along the incident laser direction is provisionally analyzed.

The lateral-direction distribution of plasma as measured in the experiments is shown in Fig. 5. From Fig. 5 we can observe that the variation of Ge XXIII ions along the incident light direction is very steep, thus causing the deviation of the X-ray laser beam from the axial line. The X-ray laser line spectrum measured with the glancing incident grating spectrograph installed at the terminal point can also verify that the X-ray laser beam deviates from the axial line of the linear plasma. Therefore, X-ray laser experiments on a thin-film target may make it easy to obtain more homogeneous gain regions compared to the thick-block plane target type of experiment.

V. Conclusions

In X-ray laser experiments, the authors utilized models closely resembling local heat equilibrium to compute the electron temperature and the relative ion abundance of germanium plasma. Moreover, the spatial resolution crystal spectrum was used to measure the axial-direction homogeneity of a linear plasma, and the lateral-direction ion distribution. At present, there are few diagnostic studies on plasma parameters in X-ray laser experiments abroad; their methods are not very mature. Generally, measurement of spectral lines relies on certain theoretical models to approximately determine the plasma parameters. Using the relative intensities of quasi-Ne ion spectral lines is more convenient [7] than the blending method and immersed-point method in directly measuring plasma parameters; moreover, it is not easy to generate the conditions affecting the production of an X-ray laser. The measurement results are basically consistent (T_e = 400 to 700 eV) with the

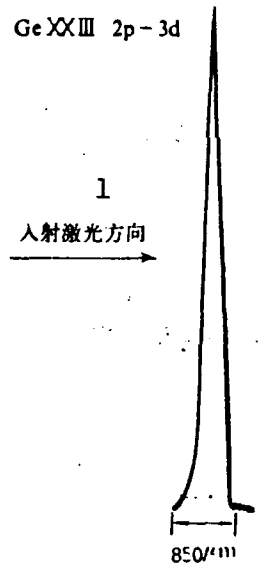

Fig. 5. Distribution status of Ge XXIII ions along the incident laser direction
KEY: 1 - direction of incident laser

measurements by the U.S. Naval Laboratory.

In the experiments, the Raman spectrograph was used to measure the electron density of the X-ray laser medium, approximately at (2 to 3) x 10^{20} /cm^3. According to the approximate adaptation conditions of PLTE, the electron density should be Ne greater than or equal to 3 x 10^{22} /cm^3 [8]. It is only an approximation in using the PLTE model in X-ray laser experiments.

In the future, a streak camera can be attached to the crystal spectrograph to conduct time resolution measurements of plasma parameters, thus obtaining the time variation properties of plasma states.

The authors express their gratitude to operational personnel

at the LF-12 laser installation for their generous assistance; the authors also thank Zhang Qiren, Zhuang Xiuqun, Du Fengying, and Zhang Tanxin for rendering valuable service.

The first draft of the paper was received on February 23, 1990; the revised draft was received for publication on April 28, 1990.

REFERENCES

1. T. N. Lee, et al. Rev. Sci. Instrument 57 (8), (1986).

2. R. C. Elton, et al. J. Opt. Soc. Am. B 4 (4), (1987).

3. Xiarg Zhilin and Yu Changxuan, Gaowen Dengliziti Zhenduan Jishu [Diagnostic Techniques of High-Temperature Plasma].

4. Hans, R. Griem, Plasma Spectroscopy (1964).

5. Chou Yanghui, "Energy level and spontaneous transition probabilities of germanium quasi-sodium, quasi-neon, and quasi-fluorine ions," (internal report).

6. Richard, A, Phys. Fluids 3 (1), (1988).

7. Rosen, M. D. et al, UCRL-52000-85-11 (1985).

8. Bekefi, G. et al, Spectroscopic Diagnostics of Laser Plasma.